Catal Lett (2008) 120:116–125
DOI 10.1007/s10562-007-9262-y

The Effects of Al_2O_3 Addition and WO_3 Modification on Catalytic Activities of NiO/TiO_2 for Acid Catalysis

Jong Rack Sohn · Sung Gyu Lee

Received: 4 July 2007 / Accepted: 31 August 2007 / Published online: 13 September 2007

Abstract $NiO/Al_2O_3–TiO_2/WO_3$ catalysts for acid catalysis were prepared by the addition of Al_2O_3 and the modification with WO_3. The strong acid sites were formed through the bonding between dispersed WO_3 and TiO_2. The larger the dispersed WO_3 amount, the higher both the acidity and catalytic activity. The addition of Al_2O_3 up to 5 mol% enhanced acidity and catalytic activity of $NiO/Al_2O_3–TiO_2/WO_3$ gradually due to the interaction between Al_2O_3 and TiO_2 and consequent formation of Al–O–Ti bond. The presence of NiO may attract reactants and enhance the local concentration of reactants near acid sites and consequently increase catalytic activity.

Keywords 2-Propanol dehydration · Cumene dealkylation · Al_2O_3 addition · WO_3 modification · Dispersed WO_3 · Acidity

1 Introduction

Many kinds of solid acids have been found: their acidic properties, their catalysis, and the structure of acid site have been elucidated and those results have been reviewed by several workers [1–4]. Solid acid catalysts are finding numerous applications in many areas. Liquid superacids based on HF, which are efficient and selective at room temperature, are not suitable for industrial processes due to separation problems tied with environmental regulations [5]. Many catalysts were reported in the literature including $AlCl_3$ with additives like $SbCl_3$ and HCl, chlorinated alumina, transition metal-exchanged zeolites, heteropoly acids and some bifunctional catalysts [6]. Most of these catalysts suffer from different drawbacks such as high working temperature, continuous supply of chlorine and a high hydrogen pressure. Conventional industrial acid catalysts, such as sulfuric acid, $AlCl_3$, and BF_3, have unavoidable drawbacks because of their severe corrosivity and high susceptibility to water. Thus the search for environmentally benign heterogeneous catalysts has driven the worldwide research of new materials as a substitute for current liquid acids and halogen-based solid acids. Among them sulfated oxides, such as sulfated zirconia, titania, and iron oxide exhibiting high thermostability, superacidic property, and high catalytic activity, have evoked increasing interest [2, 3, 7].

The cracking of hydrocarbons that are catalyzed by acid-treated clays or silica alumina, gives rise to a much different product distribution than that obtained by thermal reaction. These solid-catalyzed reactions exhibit features similar to reactions catalyzed by mineral acids. It is well known that the surface acidity of a metal oxide is improved with the incorporation of another metal oxide to form a mixed oxide catalyst. A number of combination of metal oxides generates acid sites [8–15]. A major disadvantage associated with TiO_2 support is its low specific surface area and low thermal stability of the anatase structure at high temperatures. TiO_2 alone is impractical as a catalyst because of its low catalytic activity. However, mixed oxide systems combining TiO_2 with such oxides as V_2O_5, Al_2O_3, MoO_3, P_2O_5, SiO_2, and ZnO are known to be effective for various reactions [11, 16–19].

The strong acidity of sulfated zirconia has attracted much attention because of its ability to catalyze many reaction such as cracking, alkylation, and isomerization. Recently, some workers reported zirconia or titania-supported

J. R. Sohn (✉) · S. G. Lee
Department of Applied Chemistry, Engineering College,
Kyungpook National University, Taegu 702-701, Korea
e-mail: jrsohn@knu.ac.kr

WO_3 as alternative materials in reactions requiring strong acid sites [1, 3, 20, 21]. Several advantages of tungstate over sulfate as dopant include the facts that they do not suffer from dopant loss during thermal treatment and that they undergo significantly less deactivation during catalytic reaction [21].

The search for a more active catalyst is a never ending task. At the same time that increased catalytic activity is sought, an improvement in selectivity to the desired product is also required. It is known that for titania-supported catalyst its surface area and catalytic activity are decreasing under the severe reaction condition. To overcome these deficiencies, titania was added by Al_2O_3 and was modified with WO_3 by taking advantage of high acidity, high thermal stability, and high surface area of modified TiO_2. In this paper we report new acid catalyst prepared by adding Al_2O_3 to TiO_2 and modifying TiO_2 with WO_3 for acid catlaysis. For the acid catalysis, the 2-propanol dehydration and cumene dealkylation were used as test reactions.

2 Experimental

2.1 Catalyst Preparation

The Al_2O_3–TiO_2 mixed oxide was prepared by a co-precipitation method using aqueous ammonia as the precipitation reagent. The coprecipitate of $Al(OH)_3$–$Ti(OH)_4$ was obtained by adding aqueous ammonia slowly into a mixed aqueous solution of titanium tetrachloride and aluminum nitrate(Junsei Chemical Co.) at room temperature with stirring until the pH of the mother liquor reached about 8. $Ni(OH)_2/Al(OH)_3$–$Ti(OH)_4$ was prepared by adding aqueous ammonia slowly into a mixed solution of $NiCl_2$ solution and dried $Al(OH)_3$–$Ti(OH)_4$ with stirring until the pH of solution reached about 8. The catalysts containing various tungsten oxide contents were prepared by adding an aqueous solution of ammonium metatungstate $[(NH_4)_6(H_2W_{12}O_{40}) \cdot nH_2O]$ to the dried $Ni(OH)_2/Al(OH)_3$–$Ti(OH)_4$ powder followed by drying and calcining at high temperatures for 1.5 h in air. This series of catalysts are denoted by their weight percentage of NiO and WO_3. For example, $20NiO/5Al_2O_3$–$TiO_2/15WO_3$ indicates the catalyst containing 20 wt% NiO, and 15 wt% WO_3, and 5 mol% Al_2O_3 regarding only TiO_2.

2.2 Procedure

FTIR spectra were obtained in a heatable gas cell at room temperature using a Mattson Model GL6030E spectrophotometer. The self-supporting catalyst wafers contained about 9 mg cm^{-2}. Prior to obtaining the spectra, we heated each sample under vacuum at 100–400 °C for 1 h. Catalysts were checked in order to determine the structure of the prepared catalysts by means of a Philips X́pert-APD X-ray diffractometer, employing Ni-filtered Cu K_α radiation.

The specific surface area was determined by applying the BET method to the adsorption of N_2 at –196 °C. Chemisorption of ammonia was also employed as a measure of the acidity of catalysts. The amount of chemisorption was determined based on the irreversible adsorption of ammonia [7, 22, 23]. Thus, the first adsorption of ammonia at 20 °C and 300 Torr was followed by evacuation at 230 °C for 1 h and readsorption at 20 °C, the difference between two adsorptions at 20 °C giving the amount of chemisorprion.

2-Propanol dehydration was carried out at 160–180 °C in a pulse micro-reactor connected to a gas chromatograph. Fresh catalyst in the reactor made of 1/4 in. stainless steel was pretreated at 400 °C for 1 h in a nitrogen atmosphere. Diethyleneglycol succinate on shimalite was used as packing material of the gas chromatograph and the column temperature for analyzing the product was 150 °C. Catalytic activity for 2-propanol dehydration was represented as mol of propylene converted from 2-propanol per gram of catalyst. Cumene dealkylation was carried out at 400–450 °C in the same reactor as above. Packing material for the gas chromatograph was Bentone 34 on chromosorb W and column temperature was 130 °C. Catalytic activity for cumene dealkylation was represented as mol of benzene converted from cumene per gram of catalyst. Conversions for both reactions were taken as the average of the first to sixth pulse values.

3 Results and Discussion

3.1 Infrared Spectra of WO_3 Species

To examine the structure of tungsten oxide complex under dehydration conditions, infrared spectra of $20NiO/5Al_2O_3$–$TiO_2/15WO_3$ samples were obtained in a heatable gas cell after evacuation at different temperatures for 1 h. The in situ infrared spectra in the 900–1,100 cm^{-1} region for $20NiO/5Al_2O_3$–$TiO_2/15WO_3$ are presented in Fig. 1. The infrared single band at 1,003–1,012 cm^{-1} is due to the symmetrical W=O stretching mode of the tungsten oxide complex coordinated to the $5Al_2O_3$–TiO_2 surface [24]. As shown in Fig. 1, as evacuation temperature increases, the W=O stretching mode shifts upward from 1,003 cm^{-1} to 1,012 cm^{-1}, the band becomes sharper, and the intensity increases. The similar results have been obtained with the other samples. This shows that the dehydration changes the molecular structures and that the two-dimensional tetrahedrally

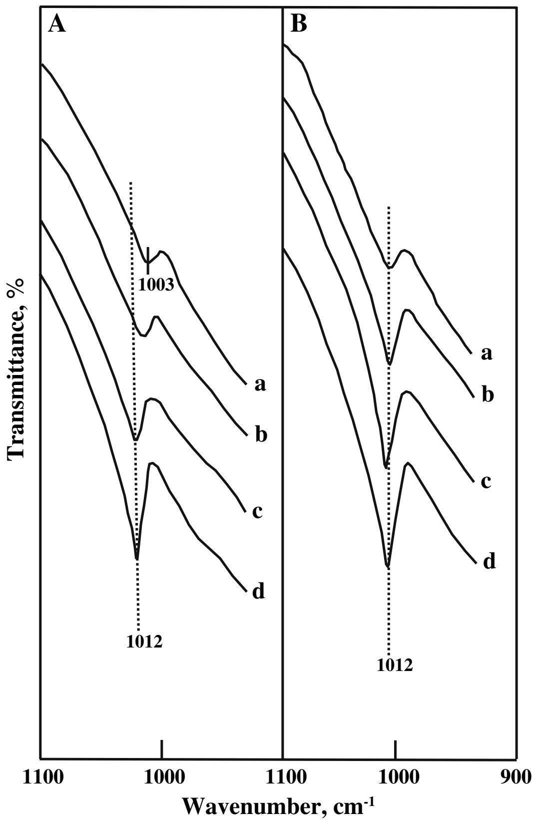

Fig. 1 (**A**) Infrared spectra of 20NiO/5Al$_2$O$_3$–TiO$_2$/15WO$_3$ evacuated at different temperatures for 1 h: (a) 100 °C (b) 200 °C (c) 300 °C and (d) 400 °C. (**B**) Infrared spectra of 20NiO/5Al$_2$O$_3$–TiO$_2$/WO$_3$ containing different WO$_3$ contents and evacuated at 400 °C for 1 h: (a) 20NiO/5Al$_2$O$_3$-TiO$_2$/3WO$_3$ (b) 20NiO/5Al$_2$O$_3$–TiO$_2$/5WO$_3$ (c) 20NiO/5Al$_2$O$_3$–TiO$_2$/10WO$_3$ and (d) 20NiO/5Al$_2$O$_3$–TiO$_2$/15WO$_3$

coordinated tungsten oxide species as well as the octahedrally coordinated polytungstate species are converted into the same highly distorted octahedrally coordinated structure as proposed for the WO$_3$/TiO$_2$ system by Wachs et al. [25]. For the other 20NiO/5Al$_2$O$_3$–TiO$_2$/WO$_3$ samples containing different WO$_3$ contents and evacuated at 400 °C the band intensity at 1,012 cm^{-1} increased with increasing the WO$_3$ content, indicating that the higher the WO$_3$ content, the more the octahedrally coordinated WO$_3$ species.

3.2 Crystalline Structures of Catalysts

The crystalline structures of catalysts calcined in air at different temperatures for 1.5 h were examined. In the case of titania support, as shown in Fig. 2, TiO$_2$ was amorphous to X-ray diffraction at 25 °C, with an anatase phase 300–400 °C, a two-phase mixture of the anatase and rutile forms at 500–600 °C, and a rutile phase at 700–800 °C. Three crystal structures of TiO$_2$, i.e., anatase, rutile, and brookite phases have been reported [26, 27]. However, in the case of 5Al$_2$O$_3$–TiO$_2$, the crystalline structures of the samples were different from the structure of pure TiO$_2$ (This figure is not shown here). 5Al$_2$O$_3$–TiO$_2$ calcined at 400 °C are mostly amorphous. The transition temperature of TiO$_2$ from amorphous to anatase phase was higher by 200 °C than that of pure TiO$_2$. X-ray diffraction data indicated only the anatase phase of TiO$_2$ at 500–800 °C, showing that the amount of anatase TiO$_2$ phase increased with increasing the calcination temperature. It is assumed that the interaction between Al$_2$O$_3$ and TiO$_2$ hinders the phase transition of TiO$_2$ from amorphous to anatase [28–30].

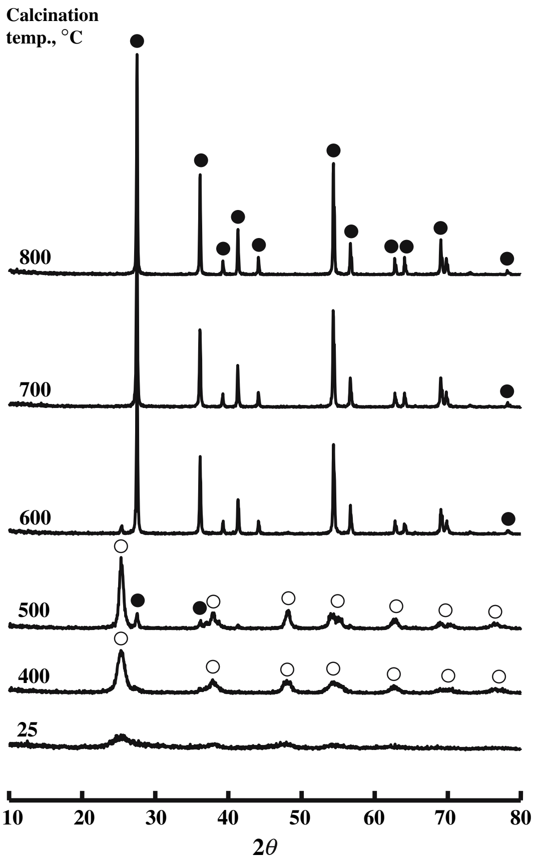

Fig. 2 X-ray diffraction patterns of TiO$_2$ calcined at different temperatures for 1.5 h: (○), anatase phase of TiO$_2$; (●), rutile phase of TiO$_2$

The XRD patterns of 20NiO/5Al$_2$O$_3$–TiO$_2$/WO$_3$ calcined at 400 °C for 1.5 h as a function of WO$_3$ content are shown in Fig. 3. WO$_3$ remained amorphous to X-ray diffraction up to 15 wt%, indicating good dispersion on the surface of catalyst. However, from 20 wt% of WO$_3$, the XRD data indicated the presence of a two-phase mixture of monoclinic phase of WO$_3$ and anatase phase of TiO$_2$, where the crystallinity of anatase phase TiO$_2$ was very poor due to the interaction between TiO$_2$ and the other oxides. In general, for the calcination temperature of 400–500 °C the hexagonal and monoclinic phases of WO$_3$ are present

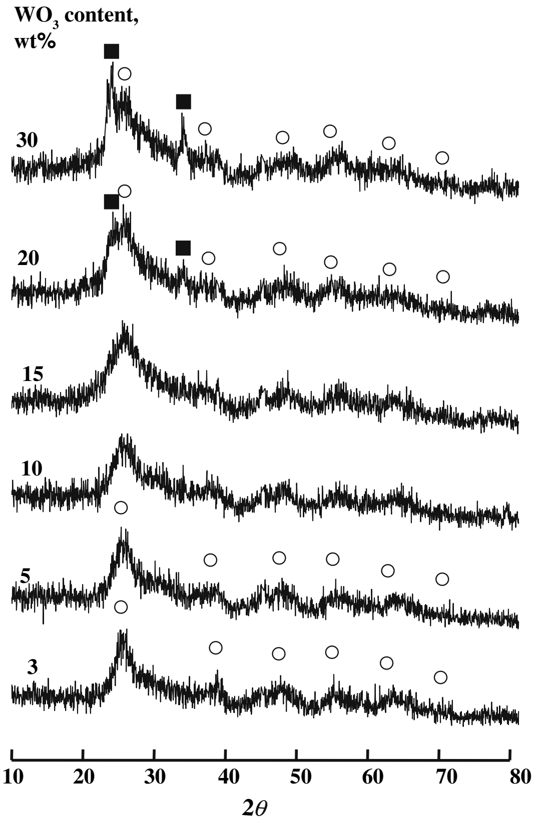

Fig. 3 X-ray diffraction patterns of $20NiO/5Al_2O_3–TiO_2/WO_3$ containing different WO_3 contents and calcined at 400 °C for 1.5 h: (○), anatase phase of TiO_2; (■), monoclinic phase of WO_3

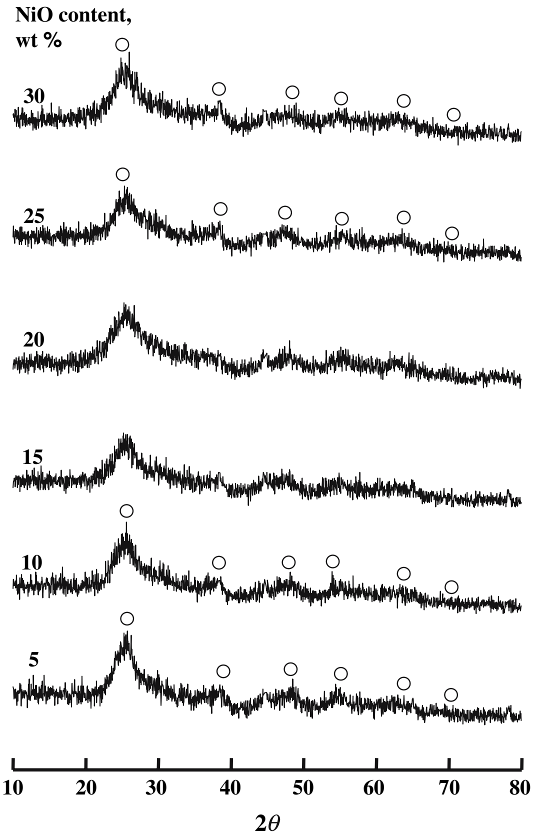

Fig. 4 X-ray diffraction patterns of $NiO/5Al_2O_3–TiO_2/15WO_3$ containing different NiO contents and calcined at 400 °C for 1.5 h: (○), anatase phase of TiO_2

[31]. However, in case of $20NiO/Al_2O_3–TiO_2/WO_3$ containing WO_3 content above 15 wt%, only the monoclinic phase of WO_3 was observed, as shown in Fig. 3.

XRD patterns of $NiO/5Al_2O_3–TiO_2/15WO_3$ calcined at 400 °C for 1.5 h as a function of NiO content are shown in Fig. 4. NiO was amorphous to X-ray diffraction regardless of NiO content up to 30 wt% of NiO, indicating excellent dispersion on the surface of catalyst. The other components, WO_3 and Al_2O_3 also remained amorphous to X-ray diffraction. In this case, also very poor crystallinity of anatase phase TiO_2 was observed due to the interaction between TiO_2 and other components. For the above Al_2O_3-promoted catalysts, there are no characteristic peaks of Al_2O_3 in the XRD patterns, implying that Al_2O_3 is sufficiently homogeneously mixed with titania.

The crystalline structures of $20NiO/5Al_2O_3–TiO_2/15WO_3$ calcined in air at different temperatures for 1.5 h were examined. As shown in Fig. 5, the catalyst was amorphous to X-ray diffraction up to 400 °C. However, for the calcination temperature of 500 °C XRD data indicated a two-phase mixture of monoclinic phase of WO_3 and anatase phase of TiO_2. The amount of two phases of TiO_2 and WO_3 increased with increasing calcination temperature, indicating that the interaction between NiO or WO_3 and TiO_2 hinders the transition of TiO_2 from amorphous to anatase phase [28, 32]. The presence of NiO and WO_3 strongly influences the development of textural properties with temperature in comparison with pure TiO_2. In fact, it is reported that for pure TiO_2 two phases of anatase and rutile TiO_2 are present at the calcination temperature of 350 °C because of no interaction of titania [32]. No phase of NiO was observed in any phase at all calcination temperature, indicating good dispersion of NiO on the surface of TiO_2 support due to the interaction between them. For the calcination temperature of 600 °C a new phase of monoclinic nickel tungstate ($NiWO_4$) was observed through the reaction between NiO and WO_3, showing that the amount of nickel tungstate increased with increasing calcination temperature, as shown in Fig. 5. For the calcination temperature of 700 °C a phase of rhombohedral nickel titanate ($NiTiO_3$) was observed newly through the reaction between NiO and TiO_2, but this phase disappeared at the calcination temperature of 800 °C due to the the decomposition of $NiTiO_3$. For the calcination temperature of 800 °C a phase transition from anatase TiO_2 to rutile TiO_2 occurred, showing the presence of a three-phase mixture of the anatase and rutile forms, and nickel tungstate.

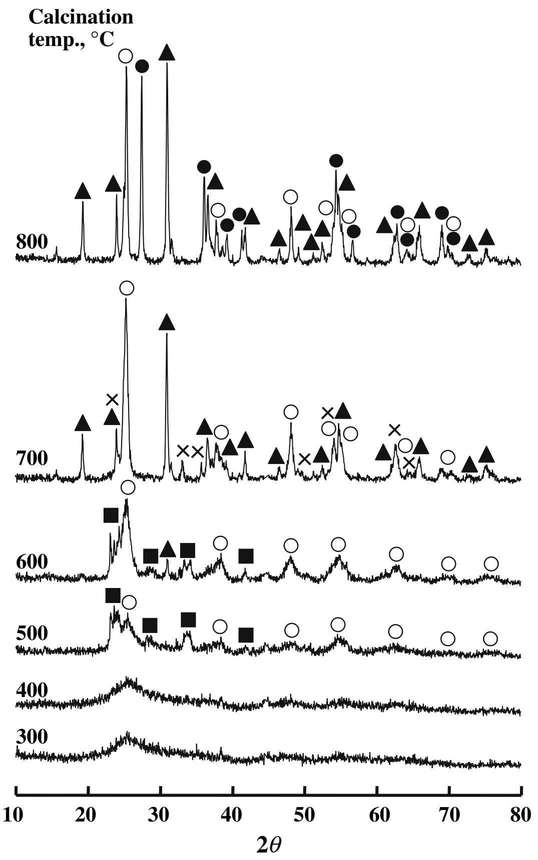

Fig. 5 X-ray diffraction patterns of $20NiO/5Al_2O_3–TiO_2/15WO_3$ calcined at different temperatures for 1.5 h: (○), anatase phase of TiO_2; (●), rutile phase of TiO_2; (■), monoclinic phase of WO_3; (▲), monoclinic phase of $NiWO_4$; (×), rhombohedral phase of $NiTiO_3$

3.3 Surface Properties

The specific surface areas of $NiO/5Al_2O_3–TiO_2/15WO_3$ catalysts containing different NiO contents and calcined at 400 °C for 1.5 h are listed in Table 1. The presence of NiO and Al_2O_3 influences the surface area in comparison with that of the pure TiO_2. Specific surface areas of $NiO/5Al_2O_3–TiO_2/15WO_3$ samples are larger than that of $5Al_2O_3–TiO_2$(93 m^2 g^{-1}) calcined at the same temperature, showing that surface area increases gradually with increasing nickel oxide loading up to 20 wt%. It seems likely that the interactions between nickel oxide (or Al_2O_3) and TiO_2 prevent catalysts from crystallizing [1]. The decrease of surface area for $NiO/5Al_2O_3–TiO_2/15WO_3$ samples containing NiO above 20 wt% is due to the blocking of TiO_2 pores by the increased NiO loading. The acidity of catalysts calcined at 400 °C, as determined by the amount of NH_3 irreversibly adsorbed at 230 °C [22, 23, 28, 33], is also listed in Table 1. The variation of acidity runs parallel to the change of surface area. The acidity increases with increasing nickel oxide content up to 20 wt% of NiO. The acidity is correlated with the catalytic activities for acid catalysis discussed below.

The specific surface areas of $20NiO/5Al_2O_3–TiO_2/WO_3$ catalysts containing different WO_3 contents and calcined at 400 °C for 1.5 h are listed in Table 2. The presence of WO_3 also influences the surface area. The surface area increases gradually with increasing tungsten oxide loading up to 15 wt%. It seems likely that the interactions between tungsten oxide (or Al_2O_3) and TiO_2 prevent catalysts from crystallizing [1]. The decrease of surface area for $20NiO/5Al_2O_3–TiO_2/WO_3$ samples containing WO_3 above 15 wt% is also due to the blocking of TiO_2 pores by the increased WO_3 loading. The acidity of catalysts calcined at 400 °C, as determined by the amount of NH_3 irreversibly adsorbed at 230 °C [22, 23, 28, 33], is also listed in Table 2. It seems likely that strong acid sites are formed through the bonding between dispersed WO_3 and TiO_2. Similarly to the case of sulfated metal oxides, the new acid sites can be formed and the acid strength can be strongly enhanced by the inductive effect of tungstate ion bonded to the surface of catalyst as follows [1, 2]:

Table 1 Specific surface area and acidity of $NiO/5Al_2O_3$-$TiO_2/15WO_3$ catalysts containing various NiO contents and calcined at 400 °C for 1.5 h

NiO content, wt%	Surface area, m^2/g	Acidity, μmol/g
0	205	204
5	260	225
10	274	232
15	281	234
20	285	247
25	272	211
30	248	203

Table 2 Specific surface area and acidity of 20-$NiO/5Al_2O_3–TiO_2/WO_3$ catalysts containing various WO_3 contents and calcined at 400 °C for 1.5 h

WO_3 content, wt%	Surface area, m^2/g	Acidity, μmol/g
0	200	192
3	257	210
5	262	213
10	269	221
15	285	247
20	236	226
30	226	220

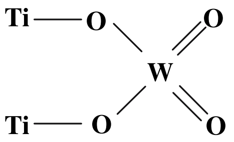

To examine the effect of WO_3 modification on the acid strength, the acid strength of the catalysts was examined by a color change method, using Hammett indicator [28, 34] in sulphuryl chloride. The $5NiO/5Al_2O_3–TiO_2/15WO_3$ sample after evacuation at 500 °C for 1 h was estimated to have $H_0 \leq -14.5$, indicating the formation of superacidic sites. However, the acid strength of $5NiO/5Al_2O_3–TiO_2$ without WO_3 was found to be $H_0 \leq -8.2$. It is very clear that the WO_3 modification gives rise to increase the acid strength of modified catalyst. Acids stronger than $H_0 \leq -11.93$, which corresponds to the acid strength of 100% H_2SO_4, are superacids [35]. Consequently, $5NiO/5Al_2O_3–TiO_2/15WO_3$ catalysts would be solid superacids. The superacidic property is attributed to the double bond nature of the W=O in the complex formed by the interaction of TiO_2 with tungstate, in analogy with the case of ZrO_2 modified with chromate and sulfate ions [30, 34].

We examined the effect of Al_2O_3 addition on the surface area and acidity of $20NiO/Al_2O_3–TiO_2/15WO_3$ samples. The specific surface areas and acidity of $20NiO/Al_2O_3–TiO_2/15WO_3$ catalysts containing different Al_2O_3 contents and calcined at 400 °C are listed in Table 3. Both surface area and acidity increased with increasing Al_2O_3 content up to 5 mol%, indicating the promoting effect of Al_2O_3 on the catalytic activities for acid catalysis described later.

Infrared spectroscopic studies of ammonia adsorbed on solid surfaces have made it possible to distinguish between Brönsted and Lewis acid sites [7, 36, 37]. Figure 6 shows the infrared spectra of ammonia adsorbed on $20NiO/5Al_2O_3–TiO_2/15WO_3$ samples evacuated at 400 °C for 1 h. For $20NiO/5Al_2O_3–TiO_2/15WO_3$, the band at 1,446 cm^{-1} is the characteristic peak of ammonium ion, which is formed on the Brönsted acid sites. The absorption peak at 1,611 cm^{-1} is contributed by ammonia coordinately bonded to Lewis acid sites [7, 36, 37], indicating the presence of both Brönsted and Lewis acid sites on the surface of $20NiO/5Al_2O_3–TiO_2/15WO_3$ sample. Other samples having different NiO and WO_3 contents also showed the presence of both Lewis and Brönsted acids.

Table 3 Specific surface area and acidity of $20-NiO/Al_2O_3–TiO_2/WO_3$ catalysts containing various Al_2O_3 contents and calcined at 400 °C for 1.5 h

Al_2O_3 content, mol %	Surface area, m^2/g	Acidity, μmol/g
0	172	182
1	193	193
2	240	230
3	250	241
5	285	247
7	269	184
10	234	161

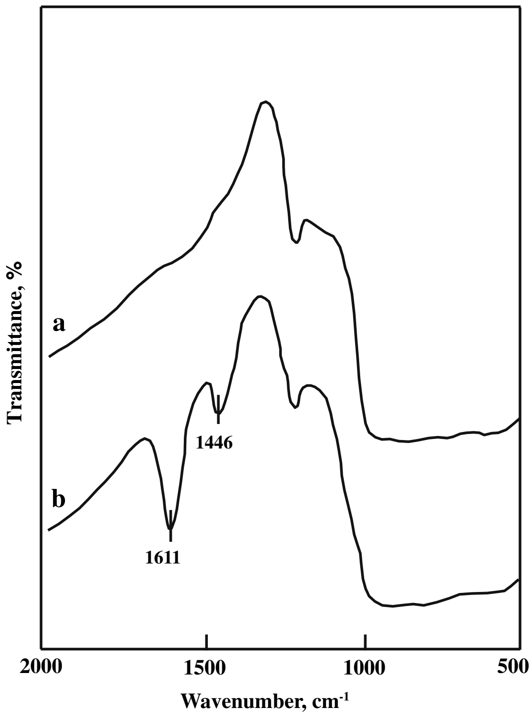

Fig. 6 Infrared spectra of NH_3 adsorbed on $20NiO/5Al_2O_3–TiO_2/15WO_3$: (a) background of $20NiO/5Al_2O_3–TiO_2/15WO_3$ after evacuation at 400 °C for 1 h, (b) NH_3 adsorbed on (a), where gas was evacuated at 230 °C for 1 h

3.4 Catalytic Activities for Acid Catalysis

3.4.1 Catalytic Activities for 2-Propanol Dehydration and Cumene Dealkylation

Catalytic activities of $20NiO/5Al_2O_3–TiO_2/15WO_3$ for 2-propanol dehydration and cumene dealkylation are plotted as a function of calcination temperature in Fig. 7. The activities for both reactions increased with the calcination temperature, reaching a maximum at 400 °C, after which the activities decreased. The decrease of activities for both reactions above 400 °C can be attributed to the fact that the surface area and acidity above 400 °C decrease with the calcination temperature. As shown in Fig. 4, for the calcination temperature above 400 °C various crystalline materials such as tungsten oxide, nickel titanate, nickel tungstate, and titania were formed and consequently the decrease of surface area and acidity gives rise to the

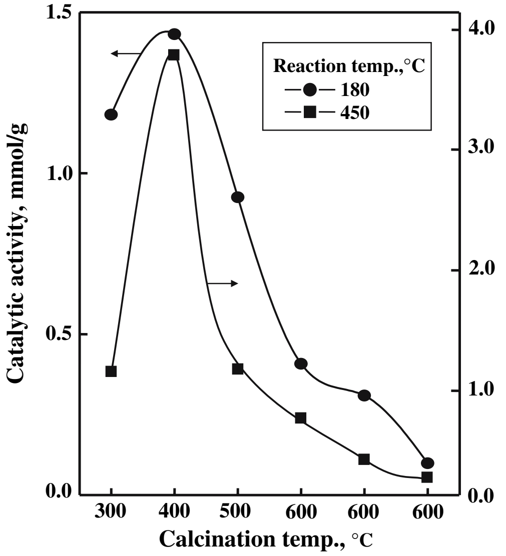

Fig. 7 Catalytic activity of $20NiO/5Al_2O_3–TiO_2/15WO_3$ for 2-propanol dehydration (●) and cumene dealkylation (■) as a function of calcination temperature

decrease of catalytic activity. Thus, in our following experiments we placed emphasis on the catalysts calcined at 400 °C.

3.4.2 Effect of NiO on Catalytic Activities

It is interesting to examine how catalytic activity of acid catalyst depends on the acid property. The catalytic activity for the 2-propanol dehydration was measured; the results are illustrated as a function of NiO content in Fig. 8, where the reaction temperature is 160–180 °C. In view of Table 1 and Fig. 8, the variation in catalytic activity for 2-propanol dehydration can be correlated with the changes of their acidity, showing the highest activity and acidity for $20NiO/5Al_2O_3–TiO_2/15WO_3$. For $NiO/5Al_2O_3–TiO_2/15WO_3$ the catalytic activity and acidity reached maxima at 20 wt% of NiO. As listed in Table 1, the presence of NiO increases the acidity, because nickel ion in NiO plays the role of Lewis acid site. Therefore, the higher the NiO content, the higher the acidity of the catalysts up to 20 wt% of NiO. The presence of NiO may attract reactants and enhance the local concentration of reactants near acid sites [33], consequently showing the increased catalytic activity. It has been known that 2-propanol dehydration takes place very readily on weak acid sites [7, 38]. Good correlations have been found in many cases between the acidity and the catalytic activities of solid acids. For example, the rates of both the catalytic decomposition of cumene and the polymerization of propylene over $SiO_2–Al_2O_3$ catalysts were found to increase with increasing acid amounts at strength $H_0 \leq +3.3$ [39]. It was also reported that the catalytic activity of nickel silicates in the ethylene demerization as well as in the butene isomerization was closely correlated with the acid amount of the catalyst [36, 40].

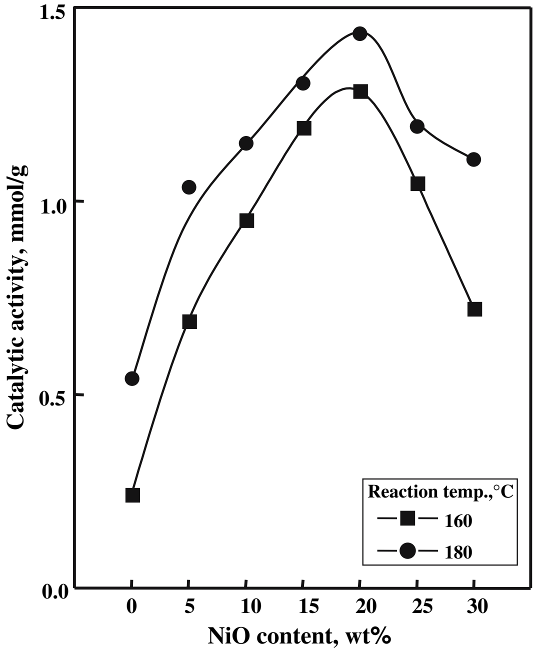

Fig. 8 Catalytic activities of $NiO/5Al_2O_3–TiO_2/15WO_3$ for 2-propanol dehydration as a function of NiO content

Cumene dealkylation takes place on relatively strong acid sites of the catalysts [38, 41]. Catalytic activities for cumene dealkylation against NiO content are presented in Fig. 9, where reaction temperature is 400–450 °C. It is

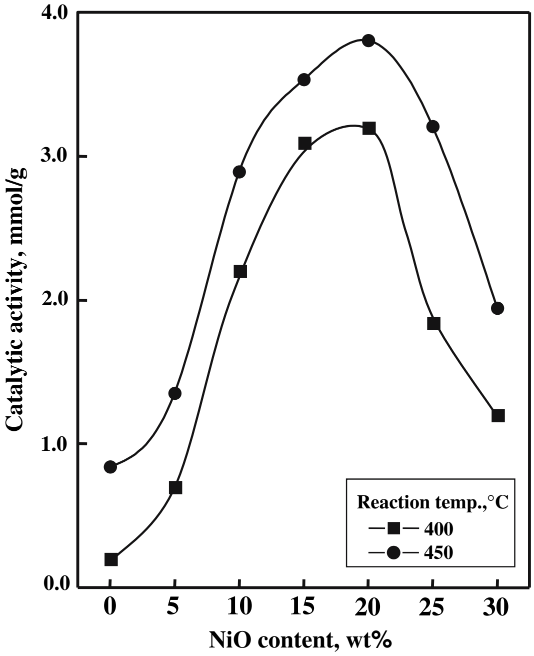

Fig. 9 Catalytic activities of $NiO/5Al_2O_3–TiO_2/15WO_3$ for cumene dealkylation as a function of NiO content

confirmed that the catalytic activity gives a maximum at 20 wt% of NiO. This seems to be closely correlated to the specific surface area and acidity of catalysts. As listed in Table 1, both BET surface area and acidity attained a maximum extent when the NiO content in the catalyst was 20 wt% and then showed a gradual decrease with increasing NiO content. The correlation between catalytic activity and acidity holds for both reactions, 2-propanol dehydration and cumene dealkylation, although the acid strength required to catalyze acid reaction is different depending on the type of reactions. As seen in Figs. 8 and 9, the catalytic activity for cumene dealkylation, in spite of higher reaction temperature, is not so higher than that for 2-propanol dehydration.

3.4.3 *Effect of WO_3 Modification on Catalytic Activities*

Recently, it has been reported that metal oxide modified with WO_3 can be used as an alternative catalyst in reactions requiring strong acid sites [3]. Several advantages of tungstate over sulfate as dopant include that it does not suffer from dopant loss during thermal treatment and it undergoes significantly less deactivation during catalytic reaction.

The catalytic activities as a function of WO_3 content is plotted in Fig. 10. As shown in Fig. 10, the maximum activity is obtained with the catalyst of 15 wt% WO_3, where the amount of dispersed WO_3 is maximum, as listed in Table 4. Therefore, it seems likely that the highest activity of the catalyst containing 15 wt% WO_3 is related to its acidity and acid strength. The high acid strength and acidity are responsible for the W=O bond nature of complex formed by the interaction between WO_3 and TiO_2 [3, 42]. Therefore, as mentioned above, the WO_3 modification resulted in the increased acid strength of modified catalyst. As discussed in IR spectra, IR spectra of $20NiO/5Al_2O_3$–$TiO_2/15WO_3$ catalyst after evacuation at 400 °C showed the band at 1,012 cm^{-1} due to the W=O stretching mode of the tungsten oxide complex bonded to the TiO_2 surface [43]. This isolated tungsten oxide species is stabilized through multiple W–O–Ti bonds between each WO_3 species and the TiO_2 surface [44, 45]. As listed in Tables 1 and 3, the acidity of $20NiO/5Al_2O_3$–$TiO_2/15WO_3$ catalyst is the most among the catalysts. Of course, the acidity of catalysts is related to their specific surface area, as mentioned above. In fact, Tables 1 and 2 show that the specific surface area attained a maximum when the WO_3 content in $20NiO/5Al_2O_3$–TiO_2/WO_3 catalysts is 15 wt%.

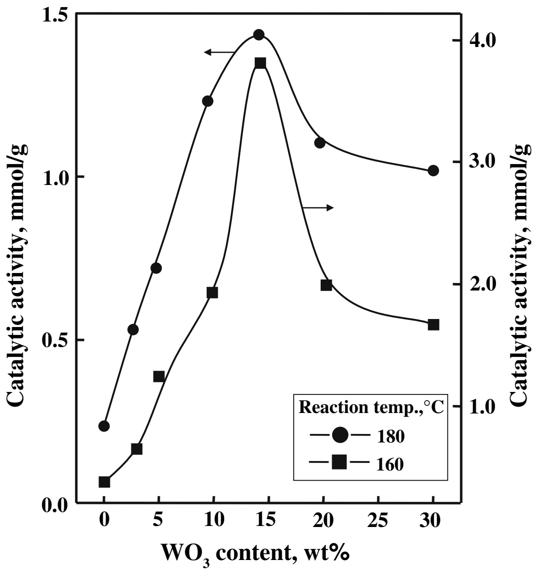

Fig. 10 Catalytic activities of $20NiO/5Al_2O_3$–TiO_2/WO_3 for 2-propanol dehydration (●) and cumene dealkylation (■) as a function of WO_3 content

The forms of active components present in heterogeneous catalysts are of importance to catalysis. A great many oxides can disperse spontaneously onto the surfaces of supports to form a monolayer, because the monolayer is a thermodynamically stable form [46]. When the loading amounts of WO_3 are low, the highly dispersed tungsten oxide species cannot be detected by XRD, as shown in Fig. 3. Therefore, we can estimate the amount of dispersed WO_3 by the quantitative XRD analysis. Dispersed WO_3 amount, surface area, acid amount, and catalytic activity for $20NiO/5Al_2O_3$–TiO_2/WO_3 catalysts containing different WO_3 contents below 20 wt% are listed in Table 4. There are good correlations among the dispersed WO_3 amount, acidity, and catalytic activity. Namely, the larger the dispersed WO_3 amount, the higher both the acidity and the catalytic activity are. This can be explained by the suggestion that strong acid sites are formed through the bonding between dispersed WO_3 and TiO_2 and consequently catalytic activity increases due to the increased acid sites.

3.4.4 *Effect of Al_2O_3 Addition on Catalytic Activities*

The catalytic activities of $20NiO/Al_2O_3$–$TiO_2/15WO_3$ as a function of Al_2O_3 content for the reaction of 2-propanol dehydration and cumene dealkylation were examined, where the catalysts were pretreated at 400 °C for 1 h before reaction; the results are shown in the Fig. 11. The catalytic activities for both reactions increased with increasing the Al_2O_3 content, reaching a maximum at 5 mol%.

Considering the experimental results of Table 3 and Fig. 11, it seems likely that the catalytic activities for both reactions closely relates to the change of acidity of

Table 4 Dispersed WO_3 amount, specific surface area, acidity, and catalytic activity for acid catalysis of $20NiO/5Al_2O_3–TiO_2/WO_3$ containing different WO_3 contents

Catalyst	Dispersed WO_3 amount [WO_3(g)/20NiO/5Al_2lO_3–TiO_2(g)]	Surface area (m^2/g)	Acidity (μmol/g)	Catalytic activity (mmol/g)	
				2-propanol dehydration	Cumene dealkylation
$20NiO/5Al_2O_3–TiO_2/0WO_3$	0	200	192	0.03	0.04
$20NiO/5Al_2O_3–TiO_2/3WO_3$	0.03	257	210	0.60	0.06
$20NiO/5Al_2O_3–TiO_2/5WO_3$	0.05	267	213	0.73	1.2
$20NiO/5Al_2O_3–TiO_2/10WO_3$	0.11	269	221	1.25	1.9
$20NiO/5Al_2O_3–TiO_2/15WO_3$	0.18	285	247	1.4	3.8

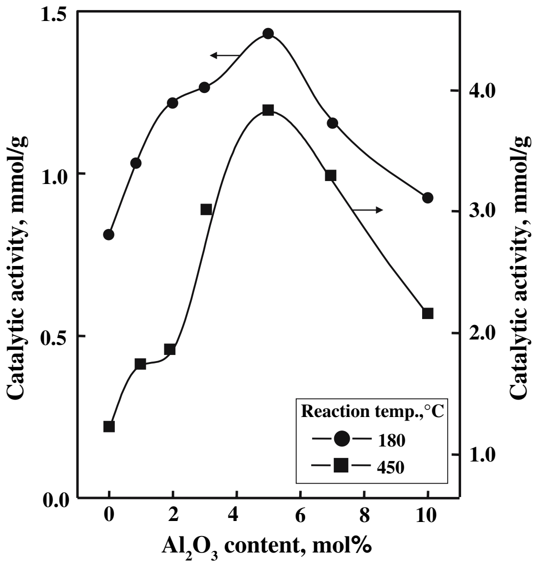

Fig. 11 Catalytic activities of $20NiO/Al_2O_3–TiO_2/15WO_3$ for 2-propanol dehydration (●) and cumene dealkylation (■) as a function of Al_2O_3 content

catalysts. As listed in Table 3, the total acid sites of $20NiO/5Al_2O_3–TiO_2/15WO_3$ and $20NiO/TiO_2/15WO_3$ are 247 μmol/g and 181 μmol/g, respectively, showing that the number of acid sites for the catalyst promoted with Al_2O_3 is greater than that for nonpromoted catalyst. This is consistent with the results reported by Hua et al. over Al_2O_3-promoted SO_4^{2-}/ZrO_2 [29]. TiO_2 alone is impractical as a catalyst because of its low catalytic activity. However, mixed oxide systems combining with other oxides are known to be effective for various reactions [11, 16–19]. Al_2O_3-promoted catalysts could be related to a strong interaction between Al_2O_3 and TiO_2. Since the promoting effect of Al_2O_3 is related to an increase in number of surface acidic sites, it would be of interest to examine various factors influencing the enhancement of these surface acidic sites.

Xia et al. [47] proposed that Al_2O_3 incorporation in TiO_2 matrix brought about an increase of the positive partial charge on the Ti cations as a result of the formation of Al–O–Ti bonds which helped to stabilize the sulfate species at the oxide surface. The formation of Al–O–Ti bond on the surface of the Al_2O_3-promoted catalysts is probably the cause for the increase in strong acidic sites. According to the principle of electronegativity equalization proposed by Sanderson [48], since the electronegativity of Al^{3+} is larger than that of Ti^{4+}, the positive charge on Ti atom is increased as a result of the formation of Al–O–Ti bond, which generates stronger acidity on these sites [29]. At the same time, the stronger Al–O–Ti bond formed by the charge transfer from Ti atom to neighboring Al atom results in an increase in the thermal stability of the surface tungstate species and consequently the acidity of Al_2O_3-promoted catalyst is increased.

3.4.5 Correlation Between Catalytic Activity and Acidity

Catalytic activities of several $NiO/Al_2O_3–TiO_2/WO_3$ catalysts containing different NiO, Al_2O_3, and WO_3 contents for both 2-propanol dehydration and cumene dealkylation were plotted as a function of acidity in Fig. 12. This shows good correlations between the catalytic activities and the acidity. This demonstrates that the catalytic activities of $NiO/Al_2O_3–TiO_2/WO_3$ essentially run parallel to the acidity. The correlation between catalytic activity and acidity holds for both reactions, 2-propanol dehydration and cumene dealkylation, although the acid strength required to catalyze acid reaction is different depending on the type of reactions. As seen in Figs. 10 and 11, the catalytic activity for cumene dealkylation, in spite of higher reaction temperature, is not so higher than that for 2-propanol dehydration.

4 Conclusions

Strong solid acid catalysts, $NiO/Al_2O_3–TiO_2/WO_3$ were prepared by adding Al_2O_3 to TiO_2 and modifying TiO_2

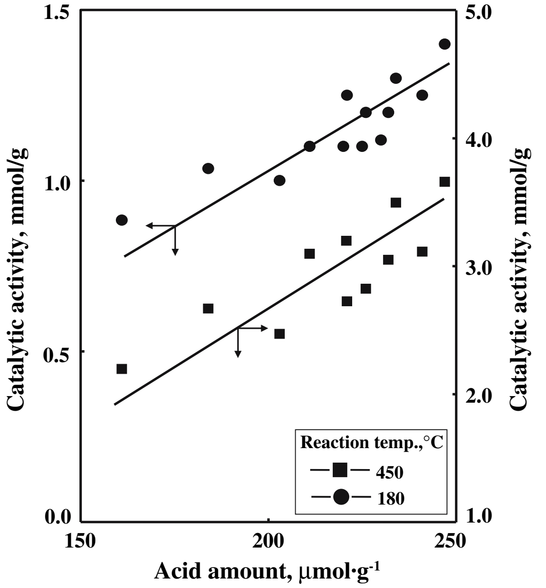

Fig. 12 Catalytic activities of $NiO/Al_2O_3–TiO_2/WO_3$ catalysts containing different NiO, Al_2O_3, and WO_3 contents for 2-propanol dehydration (●) and cumene dealkylation (■) as a function of acidity

with WO_3 for acid catalysis of 2-propanol dehydration and cumene dealkylation. $20NiO/5Al_2O_3–TiO_2/15WO_3$ containing 20 wt% NiO, 15 wt% WO_3 and 5 mol% Al_2O_3, and calcined at 400 °C, exhibited maximum catalytic activities for 2-propanol dehydration and cumene dealkylation. The catalytic activities for both reactions were correlated with the acidity of catalysts measured by an ammonia chemisorption method. The strong acid sites were formed through the bonding between dispersed WO_3 and TiO_2. The larger the dispersed WO_3 amount, the higher both the acidity and catalytic activity. The addition of Al_2O_3 up to 5 mol% enhanced acidity and catalytic activity of $NiO/Al_2O_3–TiO_2/WO_3$ gradually due to the interaction between Al_2O_3 and TiO_2 and consequent formation of Al–O–Ti bond. The presence of NiO may attract reactants and enhance the local concentration of reactants near acid sites and consequently increase catalytic activity.

Acknowledgments This work was supported by Korea Sanhak Foundation in 2006. We wish to thank Korea Basic Science Institute (Daegu Branch) for the use of X-ray diffractometer.

References

1. Sohn JR (2004) J Ind Eng Chem 10:1
2. Tanabe K, Misono M, Ono Y, Hattori H (1989) New solid acids and bases. Elsevier Science, Amsterdam, Chapter 4
3. Arata K (1990) Adv Catal 37:165
4. Davis BH, Keogh RA, Srinivasan R (1994) Catal Today 20:219
5. Olah GA, Prakash GKS, Sommer J (1985) Superacids. Wiley-Interscience, New York, USA, pp 33–52
6. Ono Y (2003) Catal Today 81:3
7. Sohn JR, Lee SH (2004) Appl Catal A: Gen 266:89
8. Bosman HJM, Kruissink EC, van der Spoel J, van der Brink F (1994) J Catal 148:660
9. Davis RJ, Liu Z (1997) Chem Mater 9:2311
10. Sohn JR, Jang HJ (1991) J Catal 132:563
11. Sohn JR, Kim HW, Lim JS (2006) J Ind Eng Chem 12:104
12. Fung J, Wang I (1996) J Catal 164:166
13. Maksimov GM, Fedotov MA, Bogdanov SV, Litvak GS, Golovin AV, Likholobov VA (2000) J Mol Catal A: Chem 158:435
14. Contescu C, Popa VT, Miller JB, Ko EI, Schwarz JA (1996) Chem Eng J 64:265
15. Scheithauer M, Grasselli RK, Knözinger H (1998) Langmuir 14:3019
16. Hucknall DJ (1974) In: selective oxidation of hydrocarbons. Academic Press, London/New York
17. Itoh M, Hattori H, Tanabe K (1974) J Catal 35:225
18. Tanabe K, Ishiya G, Ichikawa I, Hattori H (1972) Bull Chem Soc Jpn 45:47
19. Vogt ETC, Boot A, Van Dillen AJ, Geus JW, Janssen FJJG, Van der Kerkhof FMG (1988) J Catal 114:313
20. Hino M, Arata K (1987) J Chem Soc, Chem. Commun 1259
21. Larsen G, Lotero E, Para RD (1996) In: Proceedings of the 11th International Congress on catalysis. Elsevier, New York, p 543
22. Sohn JR, Park WC (2002) Appl Catal A: Gen 230:11
23. Sohn JR, Seo DH, Lee SH (2004) J Ind Eng Chem 10:309
24. Sohn JR, Park MY (1998) Langmuir 14:6140
25. Vuurman MA, Wachs IE, Hirt AM (1991) J Phys Chem 95:9928
26. G Cerrato, Marchesea L, Morterra C (1993) Appl Surf Sci 70:200
27. Alemany LJ, Berti F, Busca G, Ramis G, Robba D, Toledo GP, Trombetta M (1996) Appl Catal B: Environ 10:299
28. Sohn JR, Cho SG, Pae YI, Hayashi S (1996) J Catal 159:170
29. Hua W, Xia Y, Yue Y, Gao Z (2000) J Catal 196:104
30. Sohn JR, Cho ES (2005) Appl Catal A:Gen 282:147
31. Sohn JR, Han JS, Kim HW, Pae YI (2005) Bull Korean Chem Soc 26:755
32. Sohn JR, Lim JS (2006) Catal Lett 108:71
33. Sohn JR, Choi HD, Shin DC (2006) Bull Korean Chem Soc 27:821
34. Sohn JR, Ryu SG (1993) Langmuir 9:126
35. Olah FGA, Prakash GKS, Sommer J (1979) Science 206:13
36. Sohn JR, Park WC (2003) Appl Catal A: Gen 239:269
37. Satsuma A, Hattori A, Mizutani K, Furuta A, Miyamoto A, Hattori T, Murakami Y (1988) J Phys Chem 92:6052
38. Decanio SJ, Sohn JR, Fritz PO, Lunsford JH (1986) 101:132
39. Tanabe K (1970) Solid acids and bases. Kodansha, Tokyo, p 103
40. Sohn JR, Ozaki A (1980) J Catal 61:291
41. Sohn JR, Kim JG, Kwon TD, Park EH (2002) Langmuir 18:1666
42. Sohn JR, Kwon SH, Shin DC (2007) Appl Catal A: Gen 317:216
43. Litteti L, Nova I, Ramis G, DallAcqua L, Busca G, Giamello E, Forzatti P, Bregani F (1999) J Catal 187:419
44. Liu Z, Chen Y (1998) J Catal 177:314
45. Zhao B, Wang X, Ma H, Tang Y (1996) J Mol Catal A: Chem 108:167
46. Xie YC, Tang YQ (1990) Adv Catal 37:1
47. Xia Y, Hua W, Gao Z (1999) Appl Catal A: Gen 185:293
48. Sanderson RT (1976) Chemical bonds and bond energy. Academic Press, New York, p 75